

Article

# Precipitation Intensity Trend Detection using Hourly and Daily Observations in Portland, Oregon

Alexis Cooley and Heejun Chang \*

Department of Geography, Portland State University, Portland, OR 97201, USA; cooley@pdx.edu

\* Correspondence: changh@pdx.edu; Tel.: +1-503-725-3162

Academic Editors: Daniele Bocchiola, Claudio Cassardo and Guglielmina Diolaiuti

Received: 23 September 2016; Accepted: 13 February 2017; Published: 18 February 2017

**Abstract:** The intensity of precipitation is expected to increase in response to climate change, but the regions where this may occur are unclear. The lack of certainty from climate models warrants an examination of trends in observational records. However, the temporal resolution of records may affect the success of trend detection. Daily observations are often used, but may be too coarse to detect changes. Sub-daily records may improve detection, but their value is not yet quantified. Using daily and hourly records from 24 rain gages in Portland, Oregon (OR), trends in precipitation intensity and volume are examined for the period of 1999–2015. Daily intensity is measured using the Simple Daily Intensity Index, and this method is adapted to measure hourly scale intensity. Kendall's tau, a non-parametric correlation coefficient, is used for monotonic trend detection. Field significance and tests for spatial autocorrelation using Moran's Index are used to determine the significance of group hypothesis tests. Results indicate that the hourly data is superior in trend detection when compared with daily data; more trends are detected with hourly scale data at both the 5% and 10% significance levels. Hourly records showed a significant increase in 6 of 12 months, while daily records showed a significant increase in 4 of 12 months at the 10% significance level. At both scales increasing trends were concentrated in spring and summer months, while no winter trends were detected. Volume was shown to be increasing in most months experiencing increased intensity, and is a probable driver of the intensity trends observed.

**Keywords:** climate; precipitation intensity; hourly precipitation; hydrology; trend analysis

---

## 1. Introduction

Cities that seek to increase their resilience to extreme weather have a significant challenge. Climate change and new weather patterns seem to add management hurdles to an already complex process of infrastructure development and maintenance [1]. However, events like Hurricane Irene and Sandy demonstrate that resilience to these events is important since key infrastructure like communication networks can fail during extreme weather [2]. In the era of climate change, cities are faced with making decisions about infrastructure investment without knowing what future conditions these structures need to endure [3]. Some of the frameworks used to design flood prevention infrastructure like stormwater systems, such as Intensity-Duration-Frequency (IDF) storm curves are not designed to handle non-stationary climate conditions [4].

One area of future weather that affects infrastructure planning and is very likely to change in response to climate change is the intensity of precipitation [5]. Surface warming caused by increasing concentrations of greenhouse gases is expected to increase tropical water vapor and the transport of water vapor into the mid-latitudes [6]. Since the intensity of precipitation is determined in part by the saturation of ascending air parcels, increases in vapor can contribute to increased intensity [7].

If intensity increases, infrastructure to manage urban runoff may need to be expanded, but predicting what regions will experience these changes is difficult. Coupled land-atmosphere models

begin to approach this problem by downscaling precipitation forecasts from global climate models and pairing them with stormwater infrastructure models [8,9]. One hurdle to this approach is that modelled precipitation is uncertain because of the complexity of atmospheric circulation and vapor transport [10]. An alternate approach to identifying vulnerable regions is to emphasize the observational record [11,12]. Increased attention and analytic acuity in interpreting observational records can assist in detecting changes in precipitation intensity, and help target regions and infrastructure that may be at risk. This topic is the subject of this study.

Precipitation intensity is broadly defined as rainfall volume for a given time interval. Rainfall rates can be derived using many techniques depending on the application of interest. Near-term forecasting of rainfall rates may be accomplished through numerical weather predictions (NWP) that model evolving atmospheric dynamics or interpretation of radar images [13]. Given that NWP models may not be able to forecast extreme convective rainfalls, real-time derivation of rainfall rates can be made from satellite observations of storm convective processes and algorithms finely tuned to interpret these radiative patterns [14]. These precipitation retrieval techniques are based on a combination of microwave and infrared techniques such as Precipitation Evolving Technique [15], Passive Microwave–Global Convective Diagnostic [16], Advanced Technology Microwave Sensor [17], and artificial neural network [18,19]. Observations from rain gage networks can also be used to derive rainfall rate. From gage data, rainfall rates may be estimated for a maximum rain event or a specific time interval, such as yearly average [20].

Increased water vapor in the atmosphere over the last century has already been observed [21]. Since increased vapor is tied to increased intensity, it is possible changes to intensity may also already be occurring [22]. Studies of intensity have been performed, but are challenged by different methods for measuring precipitation intensity [20]. Many studies have used daily observational records to derive precipitation intensity in a given day (mm/day) [11,23,24]. These studies have found increasing trends in heavy precipitation events in the US and globally [12,20]. Attempts to synthesize the results of global precipitation studies led to the development of standard methodologies for defining intensity, such as the Simple Daily Intensity Index (SDII) [25]. However, this methodology assumes that daily scale data are used. Standardized methodologies for calculating intensity at the hourly scale are less common. Even without consistent methodology, studies using hourly observational records have been performed and similarly show increasing trends in the number of heavy precipitation events in the US [26]. While the relationship between sub-daily and daily precipitation observations has been discussed, it has not often been explored quantitatively, although excellent examples such as the study by Gutowski et al. are an exception [27]. Hourly records may be better suited for examinations of precipitation intensity because hourly data can reflect the time scale on which storm events operate [22]. Daily records can depress precipitation intensities because high precipitation events tend to be short lived [26]. In many cases, although the value of hourly data is acknowledged, it is not available [12].

In Portland, Oregon (OR) a unique sub-daily network of spatially dense rain gages is active. Comparison of daily and hourly observations from this network may help quantify how temporal scales affect precipitation intensity measurements and trend detection. To accomplish this, we used observations from 1999–2015 and calculated two different measures of precipitation intensity using the differently scaled data. The daily data were used to calculate precipitation intensity as defined by the SDII, which is essentially a ratio of the monthly totals in rainfall volume (mm) to days of rainfall (d). The hourly data were used to calculate intensity as a ratio of the monthly totals in rainfall volume (mm) to hours of rainfall (h). Portland area precipitation intensity has been shown to fluctuate in accordance with natural climate variability, so this short record cannot be used to determine long-term trends [27]. However, quantifying how daily and hourly observations influence trend detection may enhance other long-term studies by drawing attention to how scale may affect results.

Regional precipitation studies completed in the Pacific Northwest (PNW) (defined as southern British Columbia, Washington, Oregon, Idaho, and western Montana) show an increase in annual precipitation volume since the early 1900s [28,29]. In climate models looking out towards 2080, annual

mean precipitation is not expected to change substantially, but winters are expected to get wetter and summers drier [30]. With these climate forecasts in mind, a number of studies of precipitation have been conducted in British Columbia. Expectations of increased winter precipitation were not met. Results have consistently indicated an increase in heavy summer and spring events and few trends in winter [31,32]. The forecasted increases in winter precipitation are not yet apparent.

The City of Portland is located in the lower Pacific Northwest. The city has a maritime climate and receives two thirds of its annual precipitation between November and April [24]. Winter precipitation is a product of cyclonic storms generated over the Pacific and brought to the region on the North Pacific storm track [33]. Precipitation distribution is driven by topographic features and orographic lift [34]. Portland is located in the low lying Willamette Valley between the Coastal and Cascade mountain ranges, and therefore receives relatively lower precipitation—around 930 mm of rain annually (based on years 1981–2010) [35]. In a climate study of precipitation intensity from the 1970s, Portland was identified as having one of the least intense rainfalls compared to other places in the continental US [36]. With this history of low intensity precipitation, Portland may be vulnerable to high intensity precipitation events, as the area is not adapted to such events. Historically, several sections of local streams have been flooded, closing local roads [35]. In particular, there exists evidence of rising winter storms, recently evidenced by atmospheric rivers [37]. These winter storms bring substantial precipitation during a relatively short period. For example, significant floods hit the area in December 2015, with the month receiving the highest amounts of rainfall on record [38]. The frequency of nuisance flooding is projected to rise under climate change scenarios [35].

This study of precipitation intensity aims to improve the understanding of how temporal scale affects precipitation intensity measurement and trend detection. It will characterize the last decade of precipitation intensity trends in Portland, OR, look more closely at precipitation characteristics at the start of the twentieth-century, and consider how this topic may be best explored in the future. The following research questions guided this work:

- a. Is the daily or hourly scale better for trend detection in precipitation intensity?
- b. How is precipitation intensity related to volume?
- c. How does precipitation intensity magnitude differ at the daily or hourly scales?
- d. What is the relation among precipitation intensity, volume, and frequency of wet days/hours at a representative station?

## 2. Materials and Methods

We used hourly precipitation data collected from the volumetric Hydrological Data Retrieval and Alarm (HYDRA) Network, which is operated by the Bureau of Environmental Services in Portland, OR (<http://or.water.usgs.gov/precip>). Gages in the network measure volume by the number of tips the gage experiences within a five-minute interval, and each tip represents 0.254 mm of rainfall. The HYDRA Network includes rainfall records for 54 operational and retired stations. Only operational gages within the Portland City boundary were included in the analysis. For this study, gages currently in operation with at least 10 years of observations were selected. This resulted in 24 stations with records of 10 to 16 years in length. The location of the different gages is shown in Figure 1. This work uses a single observational precipitation data set to generate both hourly and daily observations. Where monthly observations were incomplete, that month was not included in the trend detection. For example, if a station had missing data for July 2005, that year was omitted from the July 1999–2015 records, resulting in one fewer data point used in trend detection. The use of significance levels addressed uncertainty created by these gaps. During the summer months, some stations recorded zero precipitation. These records also could not be included in trend detection because a zero value in the denominator of the precipitation intensity calculation resulted in a non-real number. For this reason, July and August have the greatest number of months missing in trend detection. All files were saved as comma separated values (CSVs) for processing by R v.3.0.2.

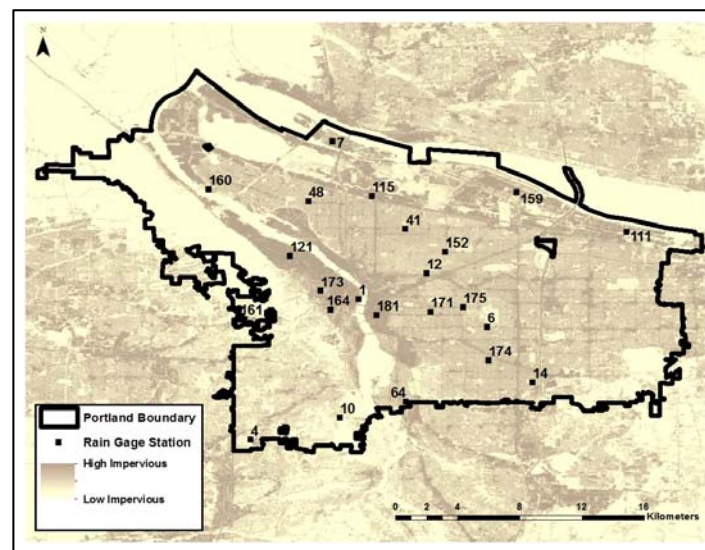


**Figure 1.** Location of weather stations in Portland, Oregon (OR).

Precipitation intensity has been measured using a number of different methods as discussed by Karl and Knight [20]. These methods include separating storm events and classifying them by frequency or magnitude to detect changes in event type over time [11,24]. Often only the largest events are of interest and an intensity threshold may be set and events beyond this threshold examined [23]. Another approach is to look at average precipitation intensity for a set time interval, such as monthly, which is the approach taken in the current study [27,39].

We calculated two different temporal resolutions of monthly precipitation intensity: daily and hourly. The calculation of daily intensity is based on the SDII climate index that has been widely adopted and used in climate research and the study of precipitation extremes [25,40]. The SDII equation is as follows:

$$SDII_j = \frac{\sum_{w=1}^W RR_{wj}}{W} \quad (1)$$

where  $RR_{wj}$  is the daily precipitation amount on wet days,  $w$ , in period  $j$ , where  $W$  represents number of wet days in  $j$ . The only modification to Equation 1 in this study is that the minimum threshold to define a wet day is lowered from 1 mm to 0.254 mm. This equation is essentially the ratio of the monthly totals in rainfall volume to the number of days when rain occurred that month (mm/day), and the same approach was taken for defining hourly scale precipitation intensity. The hourly scale precipitation intensity was calculated as the ratio of the monthly totals in rainfall volume to the number of hours when rain occurred that month (mm/hr). To allow for comparison between the two scales the units of the hourly intensity data, mm/hr, were changed to mm/day by multiplying the data by 24 (24 hours = 1 day). Each rain gage station was analyzed separately, as was each month. The result of this is that for every year of record there were 12 hourly-scale precipitation intensity measurements and 12 daily-scale precipitation intensity measurements. The critical difference between the two temporal scales is that rain events at the daily scale ranging from one to 24 hours are always recorded as having a duration of 24 hours. Because precipitation events tend to last over a number of hours rather than days, this daily-scale data can be expected to exaggerate duration and suppress precipitation intensity [22].

Monthly volume was also calculated for the 24 HYDRA stations during the period of record. This variable was selected as it is a possible factor that contributes to changes in precipitation intensity.

Once all monthly precipitation intensities and volumes were calculated, Kendall's tau was used to determine whether individual months had increasing or decreasing intensity trends during the period of record. Kendall's tau is a correlation coefficient that tests for correlation between two ranked variables [41]. The tau coefficient can be used to determine whether one variable generally increases or

decreases in concordance with a second variable. Kendall's tau was selected because it is not based on the assumption of normal distribution of either variable, and is effective in small sample sizes such as our 10–15-year periods. In addition, Kendall's tau has been widely used to detect trends in hydroclimate time-series [42,43]. The two variables used in this test were year of record and monthly precipitation intensity for a given station. Tau is scaled between  $-1$  and  $+1$ , indicating discordant or concordant correlations with the year of record variable, which is increasing. The null hypothesis was that there is no correlation between the two variables, and a p-value to determine the probability of incorrectly detecting a relationship was used to test the null hypothesis, with significance levels of 5% and 10%. Both tau and p-values were generated in R using package 'Kendall' v. 2.2 [44]. This resulted in a total of 288 tau correlation coefficients, as each of the 24 stations had one trend for each month. Kendall's p-value was used to test the significance of the trends identified at the 10% and 5% significance levels.

In order to synthesize the results of the significance tests by month and compare trend detection between scales, the concept of field significance was used. This approach provides a framework to evaluate a set of hypothesis tests, such as those used in this study where 24 stations were tested for trends in each month [45]. According to this framework, the conditions of group significance for a given month will be determined if the number of stations with significant trends is greater than the significance level applied to the total number of tests performed. This means that for a month to be significant at 5% at least two stations must be significant at 5% (e.g.,  $24 \times 0.05 = 1.2$ ) and to be significant at 10% at least three stations must be significant at 10% (e.g.,  $24 \times 0.10 = 2.4$ ).

Since Kendall's tau and field significance assume that each test is independent we used Moran's I to test Kendall's tau results for intensity and volume trends in each month for spatial autocorrelation. Moran's I is a global index of spatial autocorrelation, which we used to measure the direction and degree of spatial dependence of trends among the 24 weather stations. Similar to the aforementioned Kendall's tau correlation coefficient, Moran's I ranges from  $-1$  to  $+1$ , with 0 indicating no spatial autocorrelation (spatial randomness). A Moran's I value close to  $+1$  indicates a strongest positive spatial autocorrelation. If there is a positive spatial autocorrelation of trends among stations, precipitation trends are not spatially random, so one could erroneously reject the null hypothesis of no precipitation trends [46]. Spatial relationships were conceptualized based on inverse distance in ArcGIS 10.4.1. In field significance testing, issues of spatial autocorrelation may be corrected using Monte-Carlo simulation [47]. This study did not correct for these, so the months influenced by spatial autocorrelation may have redundant results. Limited occurrence of spatial autocorrelation suggests that the results are not redundant.

To consolidate the results of the analysis and find the general effect of the data scale on precipitation intensity magnitude, monthly averages from 1999–2015 were found for each station. A station's monthly average precipitation intensity for a given data-scale was defined as the mean monthly intensity for the station's period of record. Average monthly volume was defined as the mean monthly volume over the station's period of record.

Lastly, a case study was conducted on Station 04 to explore the relationship between volume, precipitation intensity, and frequency of wet days/hours. We found the station's average daily and hourly precipitation intensity and volume, as described above. We also identified the average frequency of wet days and hours for this station, defined as the mean monthly frequency of wet days and hours for the station's period of record. Kendall's tau was used to test the strength of correlation between pairs of the five variables at Station 04: daily precipitation intensity, hourly precipitation intensity, volume, frequency of wet days, and frequency of wet hours.

### 3. Results

#### 3.1. Daily vs. Hourly Trend Detection

The results from the Kendall's tau test of monthly precipitation intensity from 1999–2015 resulted in universally positive Kendall's tau values at both significance levels, as shown in Figure 2. Using

the hourly-scale data, precipitation intensity was found to satisfy field significance thresholds in 6 of 12 months at the 10% significance level, including March, April, May, June, July, and October (Figure 3). Using the daily-scale data, precipitation intensity satisfied significance thresholds and was found to be increasing in 4 of 12 months including, March, April, May, and July. At the 5% significance level, the hourly-scale data showed precipitation intensity increased in 5 of 12 months while the daily-scale data showed precipitation intensity increased in 3 of 12 months, as shown in Figure 4. Field significance was met in more months using the hourly scale data than the daily scale data at both significance levels.

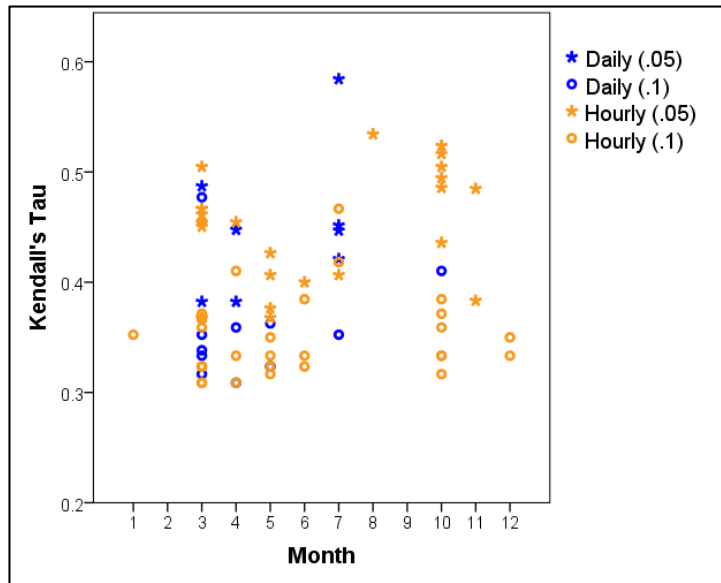


Figure 2. Kendall's Tau for precipitation intensity trends at the 10% and 5% significance levels.

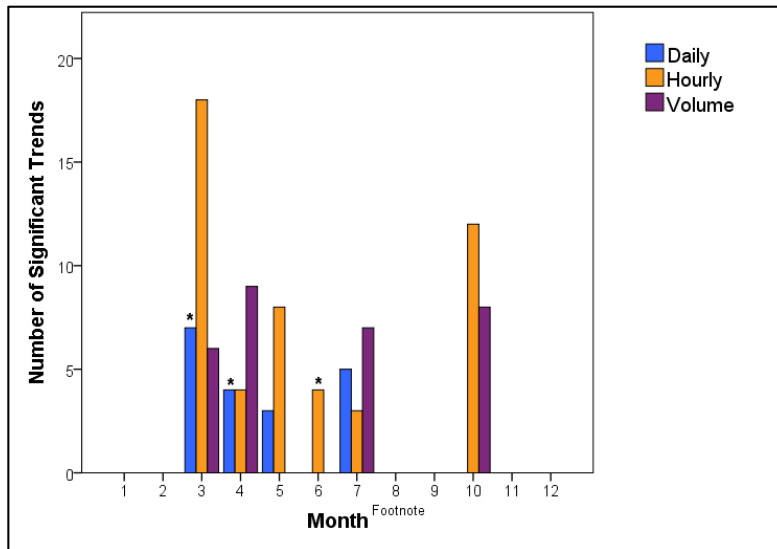
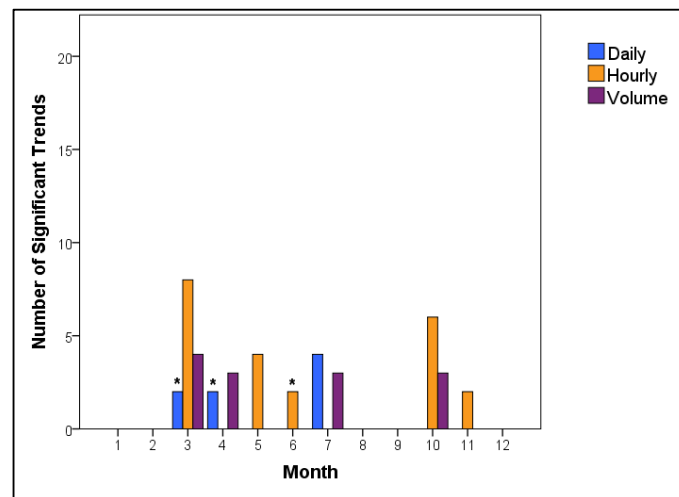


Figure 3. The number of significant trends found for months meeting field significance thresholds at 10%. \* indicates spatial autocorrelation detected for month and scale.



**Figure 4.** The number of significant trends for months meeting field significance thresholds at 5%. \* indicates spatial autocorrelation detected for month and scale.

Moran’s Index tests run on station tau values revealed that tau values were spatially autocorrelated in some months that were also field significant. Results from this test (shown in Table 1), indicate that three months exhibit both field significance and spatial autocorrelation. At the hourly scale, June has spatial autocorrelation ( $p < 0.05$ ). At the daily scale, March and April exhibit both spatial autocorrelation and field significance ( $p < 0.05$ ). August and October are also spatially autocorrelated but not field significant. The three months with autocorrelation may have trends that lack independence, possibly affecting month field significance. It is surprising that although March had many more trends that are significant at the hourly scale, spatial autocorrelation was only detected at the daily scale, as shown in Figure 5.

**Table 1.** Monthly Moran’s Index statistics. Items in bold represent months when field significance and increasing trends also occur.

	Moran’s Index											
	Jan.	Feb.	Mar.	Apr.	May.	Jun.	Jul.	Aug.	Sep.	Oct.	Nov.	Dec.
Hourly Precipitation Intensity	-	-	-	-	-	<b>0.26 **</b>	-	-	-	-	-	-
Daily Precipitation Intensity	-	-	<b>0.29 **</b>	<b>0.26 **</b>	-	-	-	0.14 *	-	0.42 **	-	-
Volume	-	-	-	-	-	-	-	-	-	-	-	-

\* Significant at the 0.1 level. \*\* Significant at the 0.05 level.

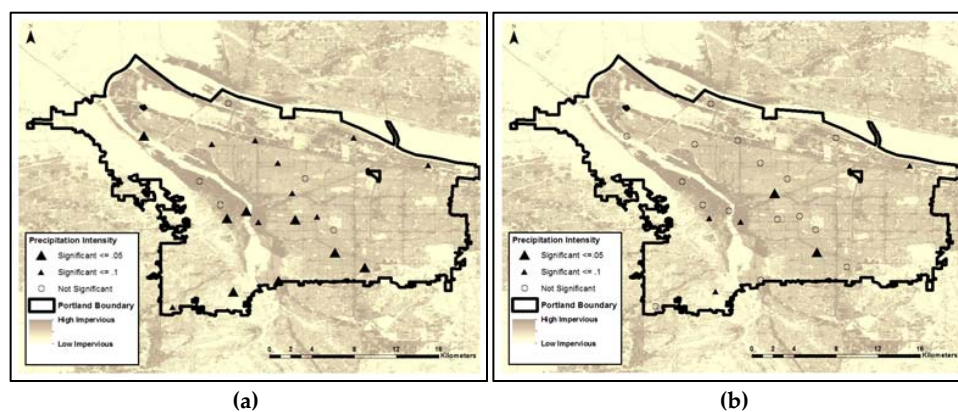


**Figure 5.** Spatial pattern of precipitation intensity trends for March (a) hourly; and (b) daily records. Spatial autocorrelation was detected in trends from daily records.

Trends concentrate in spring and summer months, and no trends are detected in winter months. At the hourly-scale, trends are clearly concentrated in March and October, so the fact that daily-scale intensity is not increasing in October is surprising. Agreement between daily and hourly-scale does become more apparent at the 10% significance level. Both scales of data resulted in trends detected in similar months (March, April, May, July). The exceptions to this are June, October, and November where trends are only in the hourly-scale data. The selection of temporal scale analysis is thus important, although the strongest trends may be apparent without regard to scale.

### 3.2. Volume Trend Detection

Results of the analysis of volume show significant increases meeting field thresholds in 4 of 12 months at both significance levels including March, April, July, and October (Figures 4 and 5). Although increasing volume is found in most seasons, no increases are found in winter months. Volume is seen as a possible driver of intensity trends, since only May and June showed increased intensity but not volume at 10% significance. All of the months that increased in volume also increased in precipitation intensity. It is not clear whether volume more closely couples with one scale of precipitation intensity over the other, because at the 5% significance level volume agrees better with daily intensity and at 10% agrees better with hourly intensity. The number of volume trends identified is roughly similar between months, and the presence of outlier months, like March and October, is missing. As shown in Table 1, Moran's Index detected no spatial autocorrelation in volume trends, so trend redundancy is not an issue. Overall, the volume results do not at this point correspond to long-term projections by global climate models that regional winters will see increased volume while summers grow drier [30].

### 3.3. Effect of Temporal Scale on Precipitation Intensity Magnitude

The daily records differ from the hourly records in the detection of sub-daily rainfall events, which has the effect of suppressing precipitation intensity values. Figure 6 shows that daily-scale March and October precipitation intensities are uniformly lower than those from hourly-scale data. Looking at the average precipitation intensity across all months (Figure 7), the same pattern is apparent. The dampening effect was detected as expected. All the precipitation intensities found using daily records are far below the hourly intensities.

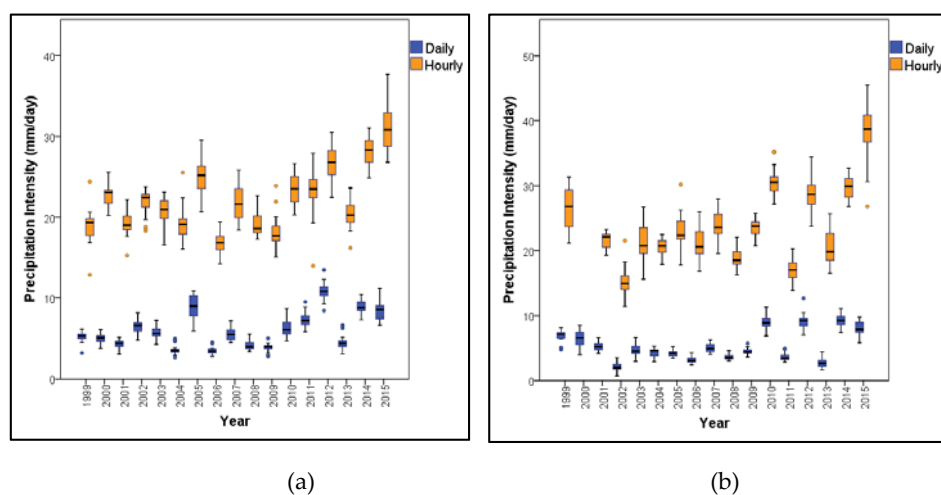


**Figure 6.** Daily and hourly precipitation intensities for all years and stations for March (a) and October (b). The box shows 50% of the data, with median represented as a black bar. The whisker extends to two standard deviations of the data, and circles represent outliers.

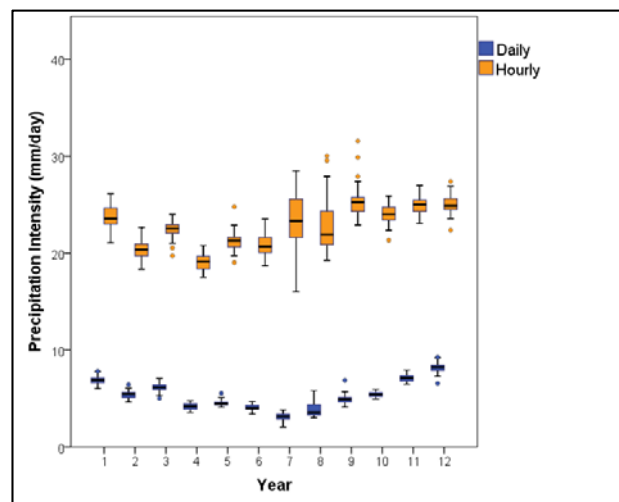


**Figure 7.** Average monthly precipitation intensity (mm/day) over the period of record for all stations for daily and hourly records. The box shows 50% of the data, with median represented as a black bar. The whisker extends to two standard deviations of the data, and circles represent outliers.

#### 3.4. Relationship between Precipitation Intensity, Volume, and Frequency of Wet Days/Hours

Visual inspection suggested there is a correlation between average daily-scale precipitation intensity (shown in Figure 7) and average volume in Figure 8. For both data sets, the minimum is July and the maximum is December. Hourly-scale precipitation intensities do not share this quality. The daily precipitation intensity appears closely coupled to volume. The case study conducted on Station 04 attempts to quantify and understand this coupling. Figures 9 and 10 show the average intensity at both scales, and the volume and wet days/hours found for Station 04. Visual inspection of these charts suggests that the correlation between daily intensity and volume is present. Testing with Kendall's tau, as shown in Figure 11, shows that daily precipitation intensity is in fact significantly and strongly correlated with volume ( $\tau = 0.91$  at 5% significance). As expected, hourly precipitation intensity is not significantly correlated with volume. Surprisingly, the frequency of wet hours, which is used in the hourly intensity calculation, does correlate significantly with volume ( $\tau = 0.81$  at 5% significance). The hourly intensity calculation is thus the only variable that exhibits independence. Variability in the frequency of wet hours that cannot be captured by the mean value is the likely reason for the independence of the hourly precipitation intensity variable.

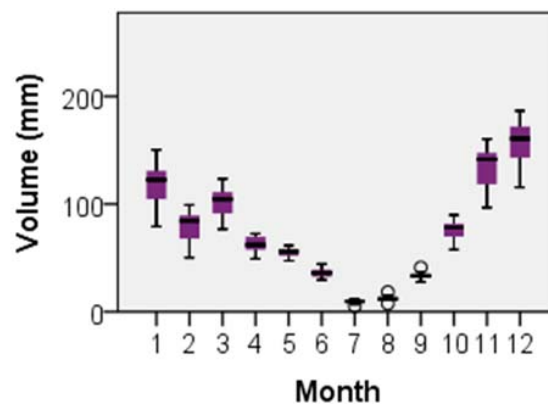


**Figure 8.** Average monthly volume (mm) over the period of record for all stations. Box shows 50% of the data, with median represented as a black bar. The whisker extends to two standard deviations of the data, and circles represent outliers.

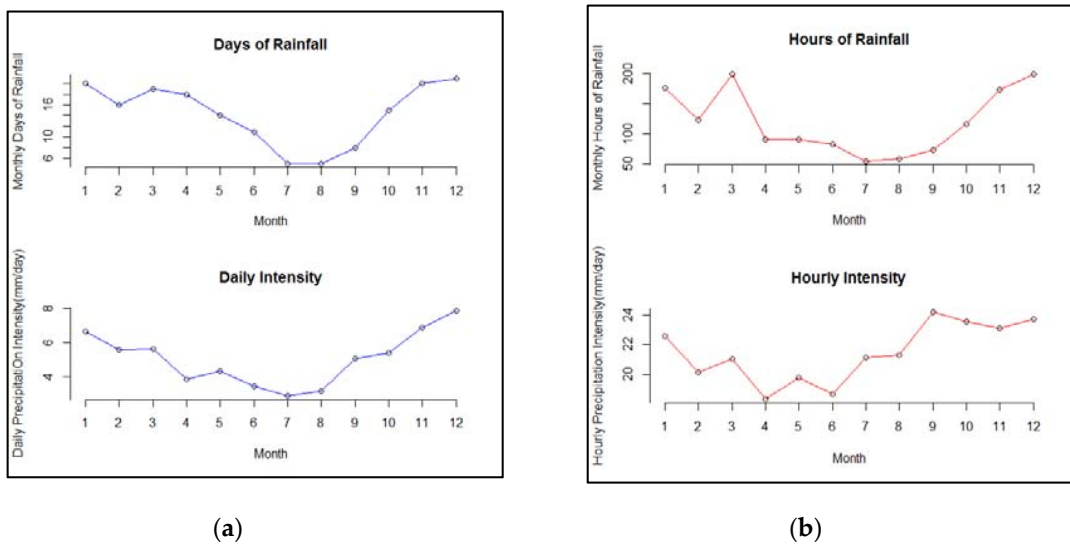


**Figure 9.** The number of wet days and daily precipitation intensity for each month, averaged for the period of 1999–2015, for Station 04 (a). The number of wet hours and hourly precipitation intensity for each month, averaged for the period of record, for Station 04 (b).

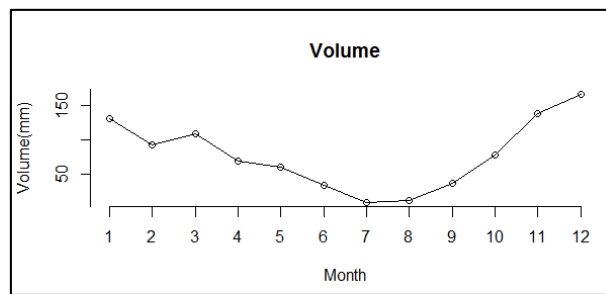


**Figure 10.** The volume on a monthly basis, averaged for the period of record, for Station 04.

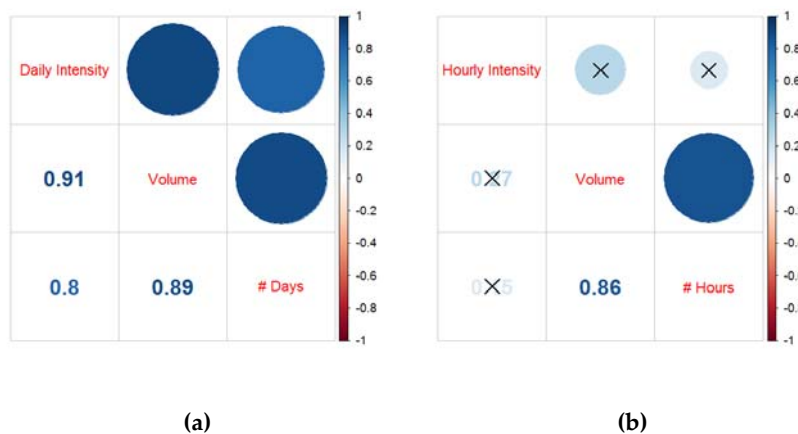


**Figure 11.** Matrixes show Kendall correlation relationships between average precipitation intensity, volume, frequency for daily (a); and hourly (b) data for Station 04. The color bar represents the Kendall tau value, and non-significant correlations at the 5 % significance level are designated with “x”.

#### 4. Discussion

Hourly observational records led to the detection of more significant trends in precipitation intensity in comparison to daily records. Considering that the climate index SDII used in this study to

measure daily intensity is widely used to assess vulnerability of water resources, these results may be of value to those interested in detecting climate changes [48,49]. Although there was considerable agreement at both scales on the months found to significantly increase in intensity, there were also gaps. For example, the month of October was not found to increase in intensity when using daily scale data. Using hourly scale data, increasing trends were overwhelmingly concentrated in this month. In 2016, a year after this study ended, the Portland region experienced the wettest October rainfall on record [50]. Examples like this might encourage continued improvement in trend detection, even while the need for standardized methodologies persists. These results reiterate comments by climatologists that sub-daily records will be valuable in monitoring the affect that climate change may have on precipitation patterns [22].

Spatial autocorrelation within the 24 stations appears to be a bigger issue when testing for trends in daily scale intensity, because one third of the months had spatial autocorrelation of tau values. This is compared with only one case of spatial autocorrelation using hourly scale precipitation intensity, and zero cases using volume. The increased spatial autocorrelation may be the result of the detection of different rainfall processes. Over short durations, rainfall is a mix of stochastic and deterministic processes, but as duration increases the deterministic elements dominate [51]. The micro-scale stochastic processes may be better represented using the hourly scale intensity, which increases the heterogeneity of the data.

Precipitation intensity is a measurement of both the frequency of wet days/hours and volume, and volume increases will drive intensity up. Increased volume was detected in most, but not all, of the months with increased precipitation intensity. Volume may be the central driver of the increased intensity that is observed, although closer examination of wet day/hours is needed to understand this completely. The preliminary analysis of wet day/hour frequency in this study suggested only that the variance of wet hours is greater than that of wet days, and did not consider how wet periods are changing with time. The higher monthly variance of wet hours may be the reason that trends are detected more in the hourly scale data, since the intensity value has a wider range which increases the potential for steepness in monotonic trends. Figures 6 and 7 show that hourly intensity has a wider range than daily intensity in most months,

Suppressed precipitation intensities were uniformly observed when using daily observations as compared to hourly, as predicted by Gutowski [26]. In order to better understand how daily versus hourly records may influence the precipitation intensities, it is useful to look closely at individual months. For example, two heavy precipitation events occurred in August and December 2015 which broke the daily volume records within their months, according to the 41-year Global Historical Climatological Network record in Portland [52]. Although the December event (61.2 mm) was far larger than the August event (14.55 mm), precipitation intensities do not necessarily reflect this, since intensity is measured for the whole month. In fact, the August hourly-scale precipitation intensity is much higher than December (57 mm/day vs. 31.08 mm/day, respectively). This is because so few hours of rain occurred in August. The hourly data are more sensitive to rain occurring during dry periods, when localized convective storms are the dominant precipitation generating mechanism. Winter months may have suppressed monthly precipitation intensity measurements because of the high frequency of rainfall. This may be the explanation why few trends were identified in winter months when frontal rain is occurring for most of the month. The precipitation intensity is flattened, making trend detection more difficult.

Neither daily intensity nor volume can supplant the value of hourly precipitation intensity. No trends in volume or daily intensity were found in months where an hourly-scale intensity trend was not also detected, at the 10% significance level. The reverse cannot be said, and both volume and daily intensity have important gaps. However, considering the relatively coarse resolution of monthly volume measurement, this variable provides a considerable bang for its buck.

Increasing precipitation intensity and volume trends were concentrated in spring (March, April, May) and summer (June, July). No winter (December, January, February) trends were detected. These

results are not consistent with climate change forecasts, but they are consistent with precipitation trends identified in multiple studies conducted in British Columbia [31,32]. This suggests that although there is not a climate change signal detected, there is regional similarity in the Pacific Northwest. The increase in spring precipitation intensity may be related to long-term analysis of Pacific Northwest precipitation where spring had the only significant long-term increasing signals in volume, while all other seasons showed mixed increasing and decreasing non-significant trends [28,29]. As mentioned earlier, it may be that the increase in spring intensity shown in this study is linked to increased volume. Cautions are needed to use the results of the study and project possible long-term trends of precipitation intensity in the future, since our analysis was based on the last 15 years of precipitation data.

The increased intensity and volume identified in this study are also likely influenced by climate variability. Oregon precipitation intensity and volume are shown to vary with climate oscillations, and correlate with ENSO and PDO phase changes [27,53]. It is unclear whether this trend will continue in the future, but as atmospheric rivers that bring heavy precipitation into the area may become more pronounced under warming scenarios, such a trend might likely to continue in the future [34]. With rising ocean sea surface temperatures, warm moist air from the Pacific Ocean could migrate further northward. This study shows the value of high resolution precipitation data such as that in Portland's HYDRA network in detecting change, even while the period of record of these datasets is limited.

It is possible to hypothesize that changes to precipitation intensity in Oregon may be an early indication of climate change, since projections do indicate a shift and intensification in the North Pacific storm track that drives Oregon's precipitation regime [27]. Downscaled climate simulations for the Pacific Northwest of North America show an increase in up to 0.3 mm in daily precipitation in the Portland area if the storm track changes [54]. However, these changes are modelled and anticipated for the end of the twenty-first century [28,29].

## 5. Conclusions

As regions confront the challenges of climate change, increased attention to meteorological records can help identify places with increasing vulnerability to extreme weather. However, the robustness of these records may set a threshold on how well trends can be detected, if at all. In order to understand the influence of data resolution on trend detection, precipitation intensity was examined in Portland, OR for the period of 1999–2015 using rain gage records from 24 stations at the hourly and daily resolution. The SDII climate indicator was used to measure daily scale intensity and a similar approach was used to measure hourly scale intensity. Changes in volume were also examined as a possible influencer. Precipitation intensity and volume were calculated as monthly averages and Kendall's tau was used to test for monotonic trends. Field significance and spatial autocorrelation with Moran's Index were used to determine monthly group significance. Results indicate that hourly scale records are superior for detecting trends. All significant trends found from both temporal resolutions were positive. These trends were concentrated in spring and summer, similar to other regional studies of precipitation intensity and volume. Most months with increasing precipitation intensity also showed increased volume, so changes to volume remain a possible driver of changes in precipitation intensity. Suppressed precipitation intensity was observed in the daily scale data, as expected, when compared with hourly-scale data.

The increased resolution of the hourly data provides additional insight to intensity trends not available at the daily scale. Further research into the effect of temporal scale on precipitation intensity trend detection is needed to better understand possible limitations of daily data measured at individual weather stations. Complimentary daily/sub-daily datasets such as the Global Precipitation Climatology Project (GPCP) and Tropical Rainfall Measuring Mission (TRMM) records may provide opportunities to further address this issue. As climatologists seek to detect changes to normal precipitation regimes, the influence of data temporal scale is an important consideration in trend detection.

**Acknowledgments:** This work was supported by the Urban Resilience to Extremes Sustainability Research Network, NSF grant number AGS-1444755. Additional support was provided by Institute for Sustainable Solutions. We appreciate three anonymous reviewers whose comments greatly improved the clarity of the manuscript. The views expressed are our own and do not necessarily reflect those of sponsoring agencies.

**Author Contributions:** Alexis Cooley and Heejun Chang conceived and designed the research; Alexis Cooley performed the statistical analyses; Alexis Cooley and Heejun Chang interpreted the results and wrote the paper.

**Conflicts of Interest:** The authors declare no conflict of interest.

## Appendix A

The significant results from Kendall’s Tau tests that were performed are given in Tables [A1–A3](#).

**Table A1.** Kendall’s Tau values for monthly precipitation intensity trends using hourly scale data.

Precipitation Intensity Trends (Hourly Scale)												
Station ID	Jan.	Feb.	Mar.	Apr.	May.	Jun.	Jul.	Aug.	Sep.	Oct.	Nov.	Dec.
1	-	-	0.45 **	-	0.33 *	-	-	-	-	0.52 **	-	-
4	-	-	0.31 *	0.31 *	-	0.33 *	-	-	-	0.37 *	-	-
6	-	-	-	-	0.38 **	-	-	-	-	0.33 *	-	-
7	-	-	-	-	-	0.32 *	-	-	-	-	-	-
10	-	-	0.47 **	0.33 *	-	-	-	-	-	0.36 *	-	-
12	-	-	0.32 *	-	0.37 **	-	-	-	-	0.49 **	-	0.33 *
14	-	-	0.37 **	-	-	-	-	-	-	-	-	-
41	-	-	0.32 *	-	-	-	-	-	-	-	-	-
48	-	-	0.32 *	-	-	-	-	-	-	-	-	-
58	-	-	-	-	0.32 *	-	0.41 **	-	-	-	-	-
64	-	-	0.37 **	-	0.32 *	-	-	-	-	0.32 *	0.38 **	-
111	-	-	0.37 *	-	0.35 *	0.40 **	-	-	-	0.50 **	-	-
115	-	-	0.31 *	-	-	-	-	-	-	0.33 *	-	-
121	-	-	-	-	-	-	-	-	-	-	-	-
152	-	-	-	-	0.43 **	-	-	-	-	-	-	0.35 *
159	-	-	0.45 *	-	-	-	0.47 *	-	-	-	-	-
160	-	-	0.47 **	-	-	0.38 *	-	-	-	-	-	-
161	-	-	0.37 *	-	-	-	-	-	-	0.49 **	-	-
164	0.35 *	-	0.50 **	-	0.41 **	-	-	-	-	0.52 **	-	-
171	-	-	0.45 **	-	-	-	0.42 *	-	-	-	-	-
173	-	-	-	0.41 *	-	-	-	0.53 **	-	-	0.48 **	-
174	-	-	0.46 **	0.45 **	-	-	-	-	-	0.44 **	-	-
175	-	-	0.36 *	-	-	-	-	-	-	0.38 *	-	-
181	-	-	0.45 *	-	-	-	-	-	-	-	-	-
Moran’s Index	-	-	-	-	-	0.26 **	-	-	-	-	-	-

\* Significant at the 0.1 level. \*\* Significant at the 0.05 level.

**Table A2.** Kendall’s Tau values for monthly precipitation intensity trends using daily scale data.

Precipitation Intensity Trends (Daily Scale)												
Station ID	Jan.	Feb.	Mar.	Apr.	May.	Jun.	Jul.	Aug.	Sep.	Oct.	Nov.	Dec.
1	-	-	-	-	-	-	-	-	-	-	-	-
4	-	-	-	-	-	-	-	-	-	-	-	-
6	-	-	-	-	-	-	-	-	-	-	-	-
7	-	-	-	-	0.32 *	-	-	-	-	-	-	-
10	-	-	0.35 *	0.45 **	-	-	-	-	-	-	-	-
12	-	-	0.38 **	-	-	-	-	-	-	-	-	-
14	-	-	-	-	-	-	0.45 **	-	-	-	-	-
41	-	-	-	-	-	-	0.35 *	-	-	-	-	-
48	-	-	-	-	-	-	-	-	-	-	-	-
58	-	-	-	-	-	-	0.42 **	-	-	-	-	-
64	-	-	0.34 *	0.38 **	-	-	-	-	-	-	-	-
111	-	-	-	0.31 *	0.32 *	-	-	-	-	-	-	-
115	-	-	-	-	-	-	-	-	-	-	-	-
121	-	-	-	-	-	-	-	-	-	-	-	-
152	-	-	-	-	-	-	-	-	-	-	-	-
159	-	-	-	-	-	-	-	-	-	-	-	-
160	-	-	-	-	-	-	-	-	-	-	-	-
161	-	-	0.32 *	-	-	-	-	-	-	-	-	-
164	-	-	0.33 *	-	-	-	-	-	-	-	-	-
171	-	-	-	-	-	-	-	-	-	-	-	-
173	-	-	-	-	-	-	0.45 **	-	-	0.41 *	-	-
174	-	-	0.49 **	0.36 *	0.36 *	-	-	-	-	-	-	-
175	-	-	-	-	-	-	0.58 **	-	-	-	-	-
181	-	-	0.48 *	-	-	-	-	-	-	-	-	-
Moran’s Index	-	-	0.29 **	0.26 **	-	-	-	0.14 *	-	0.42 **	-	-

\* Significant at the 0.1 level. \*\* Significant at the 0.05 level.

**Table A3.** Kendall’s Tau values for monthly precipitation volume.

Volume Trends												
Station ID	Jan.	Feb.	Mar.	Apr.	May.	Jun.	Jul.	Aug.	Sep.	Oct.	Nov.	Dec.
1	-	-	-	-	-	-	-	-	-	0.33 *	-	-
4	-	-	-	0.45 **	-	-	-	-	-	-	-	-
6	-	-	-	-	-	-	-	-	-	-	-	-
7	-	-	-	-	-	-	-	-	-	-	-	-
10	-	-	0.39 **	0.42 **	-	-	-	-	-	-	-	-
12	-	-	-	0.35 *	-	-	-	-	-	0.43 **	-	-
14	-	-	-	-	-	-	0.34 *	-	-	-	-	-
41	-	-	-	-	-	-	0.35 *	-	-	-	-	-
48	-	-	-	0.37 *	-	-	-	-	-	-	-	-
58	-0.33 *	-	-	0.42 **	-	-	-	-	-	-	-	-
64	-	-	0.37 **	0.31 *	-	-	-	-	-	0.35 **	-	-
111	-	-	0.37 **	0.34 *	-	-	-	-	-	0.43 **	-	-
115	-	-	-	0.33 *	-	-	-	-	-	-	-	-
121	-	-	-	-	-	-	-	-	-	-	-	-
152	-	-	-	-	-	-	-	-	-	0.35 *	-	-
159	-	-	-	-	-	-	-	-	-	-	-	-
160	-	-	0.40 **	-	-	-	-	-	-	-	-	-
161	-	0.37 *	0.37 *	0.39 *	-	-	0.39 *	-	-	-	-	-
164	-	-	0.35 *	-	-	-	-	-	-	-	-	-
171	-	-	-	-	-	-	0.41 *	-	-	-	-	-
173	-	-	-	-	-	-	0.49 **	-	-	0.41 *	-	-
174	-	-	-	-	-	-	-	-	-	-	-	-
175	-	-	-	-	-	-	0.51 **	-	-	0.38 *	-	-
181	-	-	-	-	-	-	0.51 **	-	-	0.38 *	-	-
Moran’s Index	-	-	-	-	-	-	-	-	-	-	-	-

\* Significant at the 0.1 level. \*\* Significant at the 0.05 level.

## References

1. Preston, B.L.; Mustelin, J.; Maloney, M.C. Climate adaptation heuristics and the science/policy divide. *Mitig. Adapt. Strateg. Glob. Chang.* **2015**, *20*, 467–497. [[CrossRef](#)]
2. Kwasinski, A. Effects of hurricanes Isaac and sandy on data and communications power infrastructure. In Proceedings of the 35th International Telecommunications Energy Conference 'Smart Power and Efficiency' (INTELEC), Hamburg, Germany, 13–17 October 2013.
3. Redman, C.L.; Miller, T.R. The technosphere and earth stewardship. In *Earth Stewardship*; Springer: Berlin, Germany, 2015; pp. 269–279.
4. Mailhot, A.; Duchesne, S.; Caya, D.; Talbot, G. Assessment of future change in intensity duration frequency (IDF) curves for Southern Quebec using the Canadian Regional Climate Model (CRCM). *J. Hydrol.* **2007**, *347*, 197–210. [[CrossRef](#)]
5. Trenberth, K.E. Conceptual framework for changes of extremes of the hydrological cycle with climate change. In *Weather and Climate Extremes*; Karl, T.R., Nicholls, N., Ghazi, A., Eds.; Springer: Berlin, Germany, 1999; pp. 327–339.
6. Meehl, G.A.; Arblaster, J.M.; Tebaldi, C. Understanding future patterns of increased precipitation intensity in climate model simulations. *Geophys. Res. Lett.* **2005**. [[CrossRef](#)]
7. Doswell, C.A., III; Brooks, H.E.; Maddox, R.A. Flash flood forecasting: An ingredients-based methodology. *Weather Forecast.* **1996**, *11*, 560–581. [[CrossRef](#)]
8. Semadeni-Davies, A.; Hernebring, C.; Svensson, G.; Gustafsson, L.-G. The impacts of climate change and urbanisation on drainage in Helsingborg, Sweden: Suburban stormwater. *J. Hydrol.* **2008**, *350*, 114–125. [[CrossRef](#)]
9. Rosenberg, E.A.; Keys, P.W.; Booth, D.B.; Hartley, D.; Burkey, J.; Steinemann, A.C.; Lettenmaier, D.P. Precipitation extremes and the impacts of climate change on stormwater infrastructure in Washington State. *Clim. Chang.* **2010**, *102*, 319–349. [[CrossRef](#)]
10. Chou, C.; Chen, C.-A.; Tan, P.-H.; Chen, K.T. Mechanisms for global warming impacts on precipitation frequency and intensity. *J. Clim.* **2012**, *25*, 3291–3306. [[CrossRef](#)]
11. Osborn, T.J.; Hulme, M.; Jones, P.D.; Basnett, T.A. Observed trends in the daily intensity of United Kingdom precipitation. *Int. J. Climatol.* **2000**, *20*, 347–364. [[CrossRef](#)]
12. Groisman, P.Y.; Knight, R.W.; Easterling, D.R.; Karl, T.R.; Hegerl, G.C.; Razuvaev, V.N. Trends in intense precipitation in the climate record. *J. Clim.* **2005**, *18*, 1326–1350. [[CrossRef](#)]
13. He, S.; Raghavan, S.V.; Nguyen, N.S.; Liang, S.-Y. Ensemble rainfall forecasting with numerical weather prediction and radar-based nowcasting models. *Hydrol. Process.* **2013**, *27*, 1560–1571. [[CrossRef](#)]
14. Di Paola, F.; Ricciardelli, E.; Cimini, D.; Romano, F.; Viggiano, M.; Cuomo, V. Analysis of Catania flash flood case study by using combined microwave and infrared technique. *J. Hydrometeorol.* **2014**, *15*, 1989–1998. [[CrossRef](#)]
15. Di Paola, F.; Casella, D.; Dietrich, S.; Mugnai, A.; Ricciardelli, E.; Romano, F.; SanÈ, P. Combined MW-IR Precipitation Evolving Technique (PET) of convective rain fields. *Nat. Hazards Earth Syst. Sci.* **2012**, *12*, 3557–3570. [[CrossRef](#)]
16. Casella, D.; Dietrich, S.; Paola, F.D.; Formenton, M.; Mugnai, A.; Porcu, F.; Sano, P. PM-GCD—a combined IR–MW satellite technique for frequent retrieval of heavy precipitation. *Nat. Hazards Earth Syst. Sci.* **2012**, *12*, 231–240. [[CrossRef](#)]
17. Munoz, E.A.; Di Paola, F.; Lanfri, M.; Arteaga, F.J. Observing the troposphere through the Advanced Technology Microwave Sensor (ATMS) to retrieve rain rate. *IEEE Lat. Am. Trans.* **2016**, *14*, 586–594. [[CrossRef](#)]
18. Munoz, E.A.; Di Paola, F.; Lanfri, M. Advances on rain rate retrieval from satellite platforms using artificial neural networks. *IEEE Lat. Am. Trans.* **2015**, *13*, 3179–3186. [[CrossRef](#)]
19. SanÈ, P.; Panegrossi, G.; Casella, D.; Di Paola, F.; Milani, L.; Mugnai, A.; Petracca, M.; Dietrich, S. The Passive microwave Neural network Precipitation Retrieval (PNPR) algorithm for AMSU/MHS observations: Description and application to European case studies. *Atmos. Meas. Tech.* **2015**, *8*, 837–857. [[CrossRef](#)]
20. Karl, T.R.; Knight, R.W. Secular trends of precipitation amount, frequency, and intensity in the United States. *Bull. Am. Meteorol. Soc.* **1998**, *79*, 231–241. [[CrossRef](#)]

21. Hense, A.; Krahe, P.; Flohn, H. Recent fluctuations of tropospheric temperature and water vapour content in the tropics. *Meteorol. Atmos. Phys.* **1988**, *38*, 215–227. [[CrossRef](#)]
22. Trenberth, K.E. Atmospheric moisture residence times and cycling: Implications for rainfall rates and climate change. *Clim. Chang.* **1998**, *39*, 667–694. [[CrossRef](#)]
23. Krishnamurthy, C.K.B.; Lall, U.; Kwon, H.-H. Changing frequency and intensity of rainfall extremes over India from 1951 to 2003. *J. Clim.* **2009**, *22*, 4737–4746. [[CrossRef](#)]
24. Ma, S.; Zhou, T.; Dai, A.; Han, Z. Observed changes in the distributions of daily precipitation frequency and amount over China from 1960 to 2013. *J. Clim.* **2015**, *28*, 6960–6978. [[CrossRef](#)]
25. Zhang, X.; Alexander, L.; Hegerl, G.C.; Jones, P.; Tank, A.K.; Peterson, T.C.; Trewin, B.; Zwiers, F.W. Indices for monitoring changes in extremes based on daily temperature and precipitation data. *Wiley Interdiscip. Rev. Clim. Chang.* **2011**, *2*, 851–870. [[CrossRef](#)]
26. Gutowski, W.J., Jr.; Decker, S.G.; Donavon, R.A.; Pan, Z.; Arritt, R.W.; Takle, E.S. Temporal-spatial scales of observed and simulated precipitation in central US climate. *J. Clim.* **2003**, *16*, 3841–3847. [[CrossRef](#)]
27. Praskievicz, S.; Chang, H. Winter precipitation intensity and ENSO/PDO variability in the Willamette Valley of Oregon. *Int. J. Climatol.* **2009**, *29*, 2033–2039. [[CrossRef](#)]
28. Abatzoglou, J.T.; Rupp, D.E.; Mote, P.W. Seasonal climate variability and change in the Pacific Northwest of the United States. *J. Clim.* **2014**, *27*, 2125–2142. [[CrossRef](#)]
29. Mote, P.W. Trends in temperature and precipitation in the Pacific Northwest during the twentieth century. **2003**, *77*, 271–282.
30. Mote, P.W.; Salathé, E.P., Jr. Future climate in the Pacific Northwest. *Clim. Chang.* **2010**, *102*, 29–50. [[CrossRef](#)]
31. Jakob, M.; McKendry, I.; Lee, R. Long-term changes in rainfall intensities in Vancouver, British Columbia. *Can. Water Resour. J. Rev. Can. Ressour. Hydr.* **2003**, *28*, 587–604. [[CrossRef](#)]
32. Burn, D.H.; Mansour, R.; Zhang, K.; Whitfield, P.H. Trends and variability in extreme rainfall events in British Columbia. *Can. Water Resour. J.* **2011**, *36*, 67–82. [[CrossRef](#)]
33. Dart, J.O.; Johnson, D.M. *Oregon, Wet, High and Dry*; Hapi Press: Portland, OR, USA, 1981.
34. Salathé, E.P. Comparison of various precipitation downscaling methods for the simulation of streamflow in a rainshadow river basin. *Int. J. Climatol.* **2003**, *23*, 887–901. [[CrossRef](#)]
35. Chang, H. Comparative streamflow characteristics in urbanizing basins in the Portland Metropolitan Area, Oregon, USA. *Hydrol. Process.* **2007**, *21*, 211–222. [[CrossRef](#)]
36. Jones, D.M.; Sims, A.L. Climatology of instantaneous rainfall rates. *J. Appl. Meteorol.* **1978**, *17*, 1135–1140. [[CrossRef](#)]
37. Salathé, E.P., Jr.; Hamlet, A.F.; Mass, C.F.; Lee, S.-Y.; Stumbaugh, M.; Steed, R. Estimates of twenty-first-century flood risk in the Pacific Northwest based on regional climate model simulations. *J. Hydrometeorol.* **2014**, *15*, 1881–1899. [[CrossRef](#)]
38. Ahilan, S.; Guan, M.; Sleigh, A.; Wright, N.; Chang, H. The influence of floodplain restoration on flow and sediment dynamics in an urban river. *J. Flood Risk Manag.* **2016**. [[CrossRef](#)]
39. Mearns, L.O.; Giorgi, F.; McDaniel, L.; Shields, C. Analysis of daily variability of precipitation in a nested regional climate model: Comparison with observations and doubled CO<sub>2</sub> results. *Glob. Planet. Chang.* **1995**, *10*, 55–78. [[CrossRef](#)]
40. Frich, P.; Alexander, L.; Della-marta, P.; Gleason, B.; Haylock, M.; Klein, T.A.; Tc, P. Observed coherent changes in climatic extremes during 2nd half of the 20th century. *Clim. Res.* **2002**, *19*, 193–212. [[CrossRef](#)]
41. Helsel, D.R.; Hirsch, R.M. *Statistical Methods in Water Resources Techniques of Water Resources Investigations*. U.S. Geological Survey, 2002; Book 4, Chapter A3. Available online: <https://www.epa.gov/quality/statistical-methods-water-resources-techniques-water-resources-investigations-united-states> (accessed on 12 February 2017).
42. Kendall, M.G. *Rank Correlation Measures*; Charles Griffin: London, UK, 1975.
43. Chang, H.; Jung, I.-W.; Steele, M.; Gannett, M. Spatial patterns of March and September streamflow trends in Pacific Northwest Streams, 1958–2008. *Geogr. Anal.* **2012**, *22*, 2644–2656. [[CrossRef](#)]
44. McLeod, A.I. Kendall: Kendall Rank Correlation and Mann-Kendall Trend Test. R Package Version 22. Available online: <https://cran.r-project.org/web/packages/Kendall/index.html> (accessed on 12 February 2017).
45. Livezey, R.E.; Chen, W.Y. Statistical field significance and its determination by Monte Carlo techniques. *Mon. Weather Rev.* **1983**, *111*, 46–59. [[CrossRef](#)]
46. Rogerson, P.A. *Statistical Methods for Geography: A Student's Guide*; SAGE: San Mateo, CA, USA, 2014.

47. Douglas, E.M.; Vogel, R.M.; Kroll, C.N. Trends in floods and low flows in the United States: Impact of spatial correlation. *J. Hydrol.* **2000**, *240*, 90–105. [[CrossRef](#)]
48. Limjirakan, S.; Limsakul, A.; Sriburi, T. Trends in temperature and rainfall extreme changes in Bangkok Metropolitan area. *Appl. Environ. Res.* **2010**, *32*, 31–48.
49. Wang, W.; Shao, Q.; Yang, T.; Peng, S.; Yu, Z.; Taylor, J.; Xing, W.; Zhao, C.; Sun, F. Changes in daily temperature and precipitation extremes in the Yellow River Basin, China. *Stoch. Environ. Res. Risk Assess.* **2013**, *27*, 401–421. [[CrossRef](#)]
50. National Weather Service Portland, OR Record Report. Available online: <http://w2.weather.gov/climate/getclimate.php?date=&wfo=pqr&sid=PQR&pil=RER&recent=yes&specdate=2016-10-31+11%3A55%3A10> (accessed on 2 February 2017).
51. Pathirana, A.; Herath, S. Multifractal modelling and simulation of rain fields exhibiting spatial heterogeneity. *Hydrol. Earth Syst. Sci.* **2002**, *6*, 695–708. [[CrossRef](#)]
52. Daily Weather Records | Data Tools | Climate Data Online (CDO) | National Climatic Data Center (NCDC). Available online: <https://www.ncdc.noaa.gov/cdo-web/datatools/records> (accessed on 25 August 2016).
53. Hamlet, A.F.; Lettenmaier, D.P. Columbia River streamflow forecasting based on ENSO and PDO climate signals. *J. Water Resour. Plan. Manag.* **1999**, *125*, 333–341. [[CrossRef](#)]
54. Salathé, E.P. Influences of a shift in North Pacific storm tracks on western North American precipitation under global warming. *Geophys. Res. Lett.* **2006**. [[CrossRef](#)]



© 2017 by the authors; licensee MDPI, Basel, Switzerland. This article is an open access article distributed under the terms and conditions of the Creative Commons Attribution (CC BY) license (<http://creativecommons.org/licenses/by/4.0/>).